Journal of Advanced Zoology

ISSN: 0253-7214
Volume **44** *Special Issue-***2 Year 2023** *Page* **4777:4783**

Impact of Nickel Concentration on Structural, Morphological and Optical Properties of Jet Nebulizer Spray pyrolysis Coated Ni-MoO_3 Thin Films: Evaluation of n-Ni-MoO_3/p-Si Junction Didoes

G.Lavanya [1]*, N.Sivanandan [2]

[1] Research Scholar, Department of Electronics, PSG College of Arts and Science, Coimbatore, India
[2] Assistant Professor, Department of Electronics, PSG College of Arts and Science, Coimbatore, India
[1] lavanya.gnanavelk@gmail.com, [2] sivanandan@psgcas.ac.in
*Corresponding Author E-mail: lavanya.gnanavelk@gmail.com

Article History

Received: 08 Sept 2023
Revised: 29 Oct 2023
Accepted: 05 Nov 2023

Abstract

Monoclinic structured MoO_3 thin films were prepared on a glass substrate. The Ni doped materials to add the MoO_3 in different concentrations (1%, 3%, 5%) at Wt% with MoO_3 precursor and synthesis was done using the spray pyrolysis method. X-ray diffraction revealed the incorporation of Ni in the MoO_3 Monoclinic structure. FE-SEM images showed more dispersive and rod shapes than Ni-doped MoO_3 and pure MoO_3 respectively. The ideality factor, barrier height, and saturation current were measured for two samples pure MoO_3 and Ni-doped MoO_3 at 5% doping level. The ideality factor was calculated using electrical measurements, while the barrier height and saturation current were determined through analysis of the current-voltage (I-V) characteristics.

Keywords: *Monoclinic, MoO3 thin film, spray pyrolysis, junction diode.*

1. INTRODUCTION

Transition metal oxide, remarkably MoO_3 due to its physical and chemical properties had a wide attention in research. Since last few years MoO_3 possess good structural, electronic and optical characteristics that finds its application in gas sensors, catalysts and opto electronic field [1-5]. The n-type MoO_3 films shows good results in photovoltaic applications. Among the various preparation methods available spray pyrolysis techniques is found to be the simplest and low cost method [6-8]. Which has economically attractive setups. The MoO_3 has a wide ban gap n-type material which possess good structural and electronic characteristic that can be used in many industrial applications [9-10]. The fabrication of p-Si junction diode using spray pyrolysis technique is a simple, low cost and low temperature process which has a remarkable opening for the making of photonic and nano electronic devices [11, 12]. This report presents an analysis of the ideality factor (n), barrier height (ΦB), and saturation current (Io) for two different samples: pure MoO_3 and Ni-doped MoO_3 at a 5% doping level. These parameters play a crucial role in understanding the electrical behavior of semiconductor materials. The ideality factor reflects the degree of deviation from the ideal diode behavior, the barrier height represents the energy barrier that charge carriers must overcome, and the saturation current provides insights into the leakage current across the material.

2. RESULTS AND DISCUSSION

XRD Analysis:

Figure 1 shows the XRD pattern of prepared samples of pure and Ni doped MoO_3 thin films using the jet nebulizer spray pyrolysis technique at 450˚C. Figure 1 shows XRD all detectable peaks (0 0 1, 1 0 0, 0 0 2, 0 1 1, 1 1 0, 0 1 2, 1 0 2, 2 0 1, 0 2 0, 1 2 0, 2 1 1) can be indexed to Pure MoO_3 monoclinic structure with JCPDS card no. 85-2405. The monoclinic lattice parameter, the values of *d*, the distance between the crystal planes, were calculated from Bragg Law, $\lambda=2d\sin\theta$. Table 1 shows the Structural parameter of MoO_3 and Ni doped MoO_3 (1%, 3% and 5%). The (2 2 1) (*h k l*) plane was selected to calculated the structural parameters of the prepared the samples [13-17].

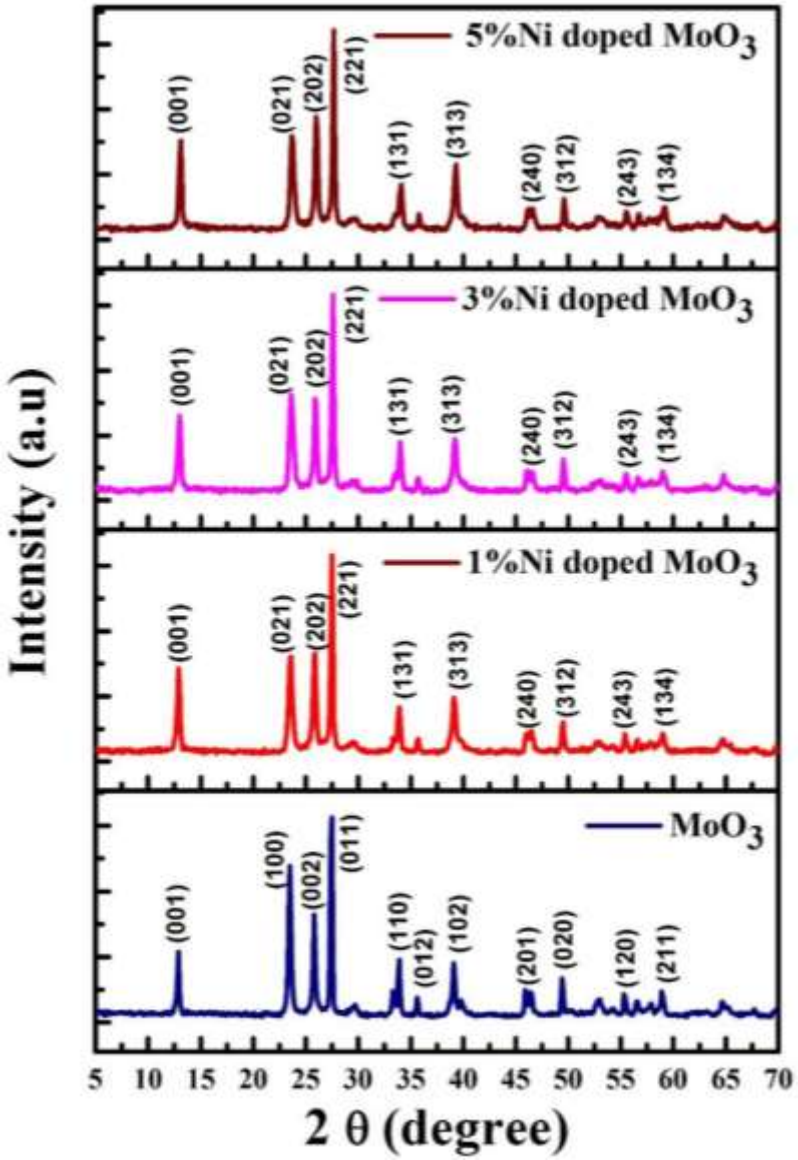

Figure 1. XRD pattern of MoO_3 and Ni doped MoO_3 (1%, 3% and 5%)

Table 1. Structural parameter of MoO_3 and Ni doped MoO_3 (1%, 3% and 5%)

Material	**Diffraction Angle 2θ**	**(221) Inter planar distance Å**	**FWHM (Radians)**	**Crystallite size (*D*) nm**	**Micro strain (ε) (× 10 −3 lines− 2 m−4)**	**Dislocation density (× 1014 lines/m2)**	**Stacking fault × 10–2**
Pure MoO_3	27.4330	3.24859	0.27250	52.41	3.639	0.0661	0.14915
1% Ni doped MoO_3	27.4848	3.24259	0.28080	50.87	3.863	0.0681	0.15386
3% Ni doped MoO_3	27.5702	3.23274	0.28820	49.57	4.068	0.0699	0.15820
5% Ni doped MoO_3	27.6417	3.22454	0.29520	48.40	4.267	0.07166	0.16229

FE-SEM Analysis:

Figure 2 displays the analyzed MoO_3 films as well as the thin film samples of Ni-doped MoO_3 at concentrations of 1%, 3%, and 5%. These samples underwent examination using low magnification (2µm) via FE-SEM analysis. In Figure 2a, visuals of multidispersive and unevenly sized rods are apparent. Upon introducing 1%, 3%, and 5% Ni doping into the MoO_3 samples, the images reveal a higher degree of dispersion and rod-like formations compared to pure MoO_3. The imagery illustrates a notable alteration in the shapes of the prepared samples, coinciding with an increase in doping concentration, which in turn contributes to a more loosely defined surface tension.

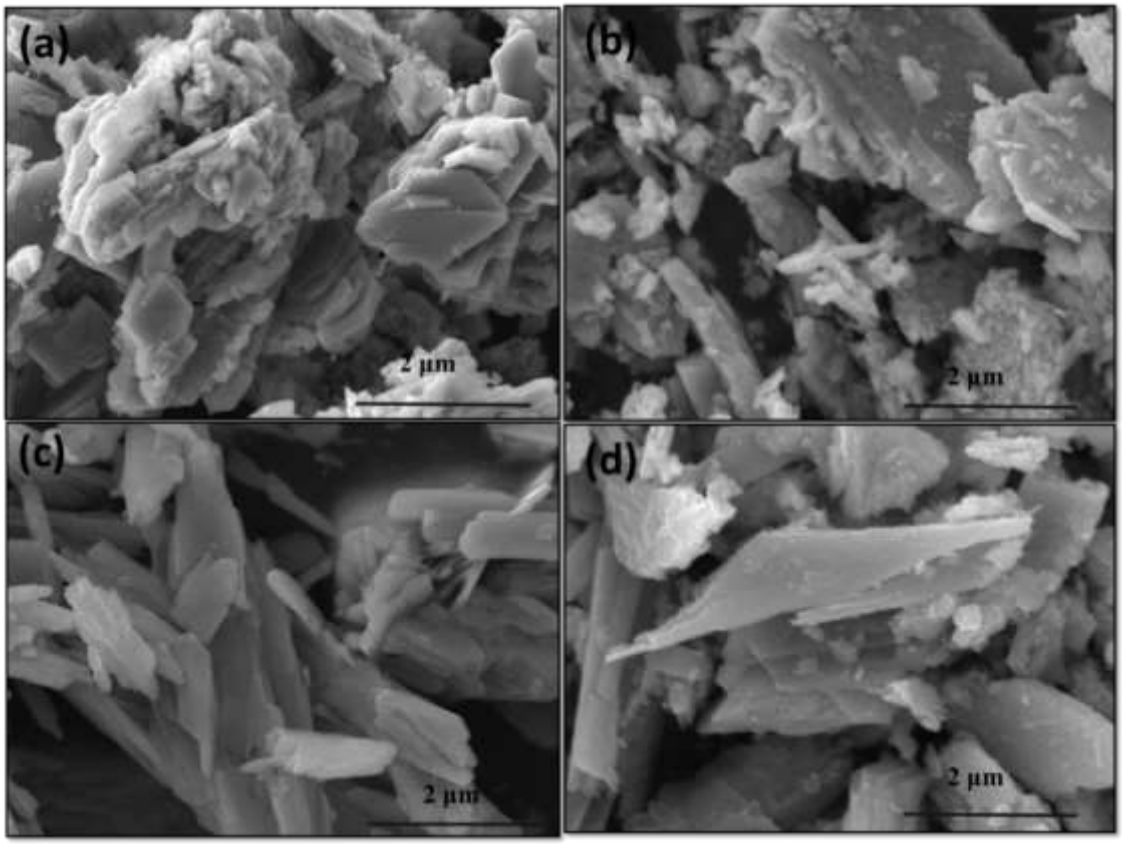

Figure 2. FE-SEM images of MoO_3 and Ni doped MoO_3 (1%, 3% and 5%)

Elemental Analysis

Figure 3 shows the EDAX spectrum of MoO_3 and Ni doped MoO_3 (1%, 3% and 5%). According to the data presented in Table 2 (a), the elemental analysis spectrum for pure MoO_3 unequivocally demonstrates the presence of Mo and O elements in the prepared samples, with no detectable indication of other elements [18, 19]. In Table 2 (b-d), the elemental analysis spectrum for Ni-doped MoO_3 illustrates the existence of Ni, Mo, and O elements within the samples that were prepared.

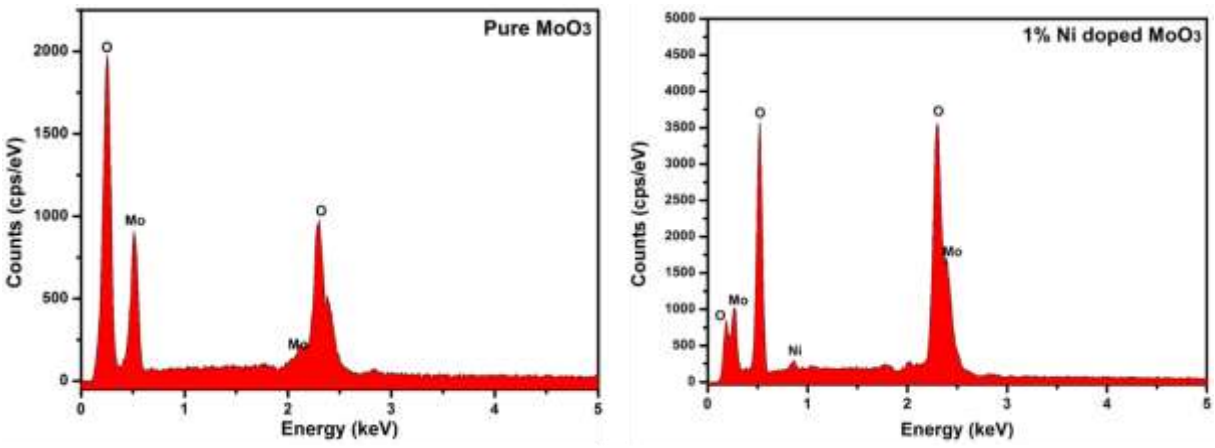

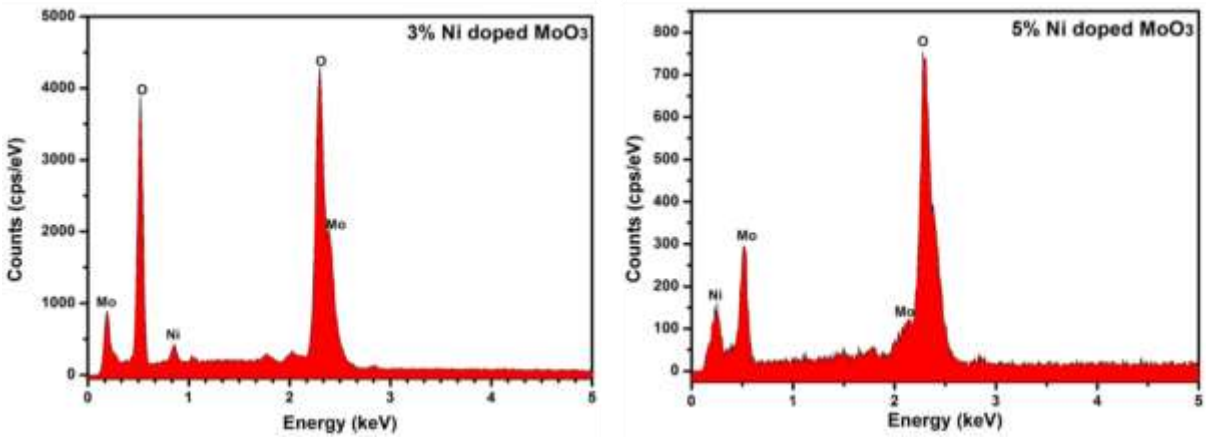

Figure 3. EDAX of MoO_3 and Ni doped MoO_3 (1%, 3% and 5%)

Table 2. Elemental analysis of MoO_3 and Ni doped MoO_3 (1%, 3% and 5%)

(a)

Elements	Weight %	Atomic %
O k	35.68	75.82
Mo L	64.32	24.18

(b)

Elements	Weight %	Atomic %
O k	28.57	72.01
Ni L	1.98	1.28
Mo L	69.45	26.71

(c)

Elements	Weight %	Atomic %
O k	29.82	70.63
Ni L	2.83	2.42
Mo L	67.35	26.95

(d)

Elements	Weight %	Atomic %
O k	26.92	69.32
Ni L	3.24	3.01
Mo L	69.84	27.67

UV-Vis Analysis

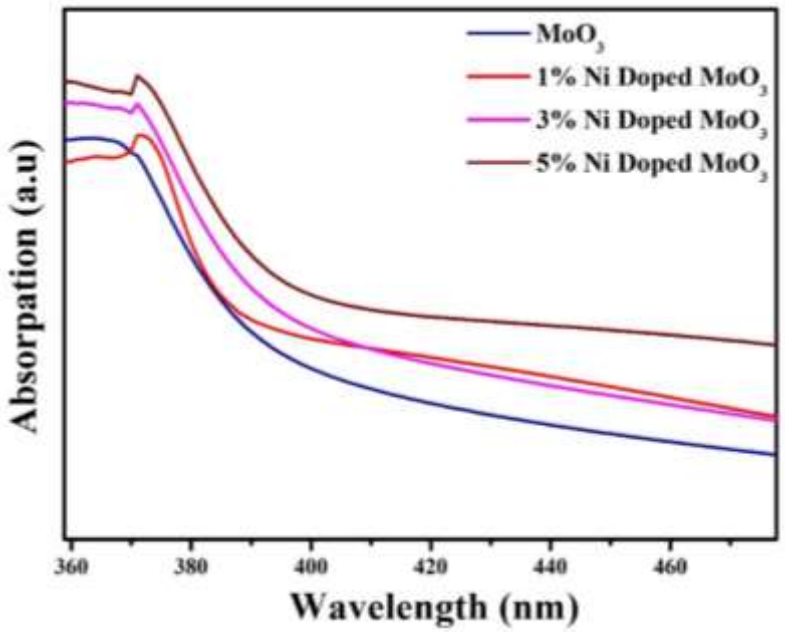

Figure 4. UV-Vis analysis of MoO_3 and Ni doped MoO_3 (1%, 3% and 5%)

Figure 4 shows the UV-Vis analysis spectrum of Pure and doped MoO_3. Compared with Pure MoO_3, 1%, 3%, and 5% Ni doped MoO_3 were peak observed 363 nm, 370 nm, 372 nm, 375 nm respectively.

I-V characteristics of n-Ni doped MoO_3/p-Si diodes

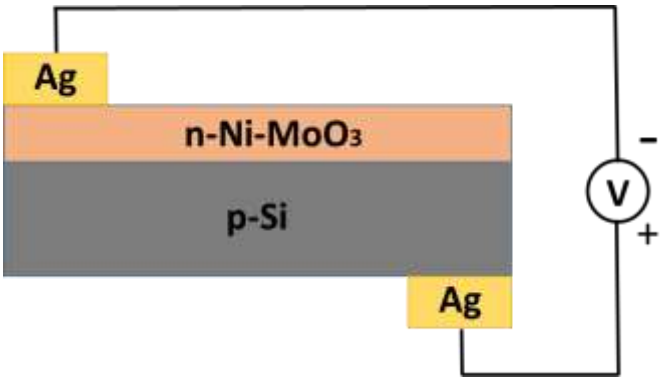

Fig. 5(a) The device structure of back contact

Fig.5 (a) shows represents the schematic of n-MoO_3/ p-Si device structure the current voltage characteristics of undoped and Ni (wt.5%) doped n-MoO_3/p-Si diode.

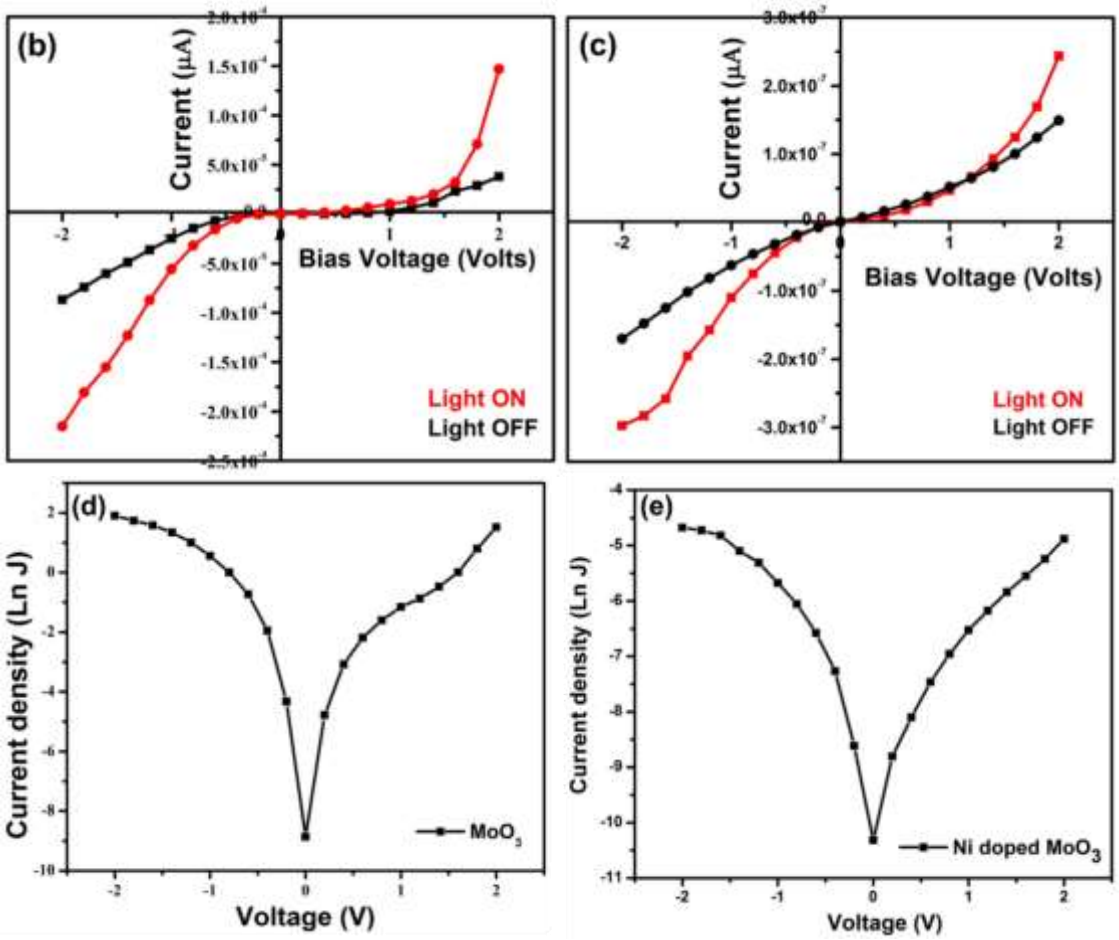

Fig. 5. (b - d). I-V curve of (b) n-MoO_3/p-Si, (d) n-Ni MoO_3/p-Si diodes, I-V curve of (c, e) current density (J)-voltage (V) plots of pure MoO_3 and n-Ni MoO_3/p-Si diodes

Figure 5 depicts the I-V curve of n-MoO3/p-Si, (d) n-Ni MoO3/p-Si diodes and current density (J)-voltage (V) plots of pure MoO3 and n-Ni MoO3/p-Si diodes.

For pure MoO_3, the ideality factor (n) was measured to be approximately 1.5744. In the case of Ni-doped MoO_3 at 5% doping, the ideality factor increased significantly to around 4.1864. The increase in the ideality factor for the doped sample suggests the presence of additional recombination centers or defects in the material. This deviation from the ideal value of 1 indicates a less ideal diode behavior, potentially due to the incorporation of Ni impurities. The barrier height (ΦB) represents the energy difference between the conduction band edge and

the Fermi level, indicating the ease with which charge carriers can move across the semiconductor junction [20, 21]. For pure MoO_3, the barrier height was calculated to be approximately 0.41702 eV. With Ni doping at 5%, the barrier height increased to around 0.58584 eV. The increase in barrier height with doping could be attributed to changes in the electronic structure of the material due to Ni incorporation, affecting charge carrier transport. Saturation current (Io) signifies the leakage current when the diode is in the reverse-biased condition and provides information about the material's quality and purity. Pure MoO_3 exhibited a saturation current of 5.42×10^{-5} A. Ni-doped MoO_3 at 5% doping showed a significantly lower saturation current of 8.96×10^{-8} A. The lower saturation current in the doped sample suggests improved material quality, possibly due to the reduction in defects or impurities at the semiconductor interface [22].

3. CONCLUSION

Pure MoO_3 and Ni-doped MoO_3 thin films were made coated successfully and characterized using simple and rapid synthesized method. The analysis of ideality factor, barrier height, and saturation current for pure MoO_3 and Ni-doped MoO_3 (5% doping) revealed distinct differences in the electrical behavior of the two samples. The increased ideality factor, higher barrier height, and lower saturation current observed in the doped sample suggest the influence of Ni doping on the electronic properties of MoO_3. Further investigations into the role of doping and its impact on the semiconductor behavior are warranted to gain a comprehensive understanding of the material's electrical characteristics.

References

G. Wang, T. Jiu, P. Li, J. Li, C. Sun, F. Lu, J. Fang, Preparation and characterization of MoO3 hole-injection layer for organic solar cell fabrication and optimization. Sol. Energy Mater. Sol. Cells 120, 603–609 (2014)

Q. Fu, J. Chen, C. Shi, D. Ma, Room-temperature sol–gel derived molybdenum oxide thin films for efficient and stable solution-processed organic light-emitting diodes. ACS Appl.Mater. Interfaces. https://doi.org/10.1021/am4007319.

R. Pandeeswari, B.G. Jeyaprakash, Nanostructured α-MoO3 thin flm as a highly selective TMA sensor. Biosens. Bioelectron. (2013). https://doi.org/10.1016/j.bios.2013.09.057

T.N. Lin, Y.H. Lin, C.T. Lee, S. Han, K.W. Weng, Electrochromic properties of bipolar pulsed magnetron sputter deposited tungsten-molybdenum oxide films. Thin Solid Films (2015).https://doi.org/10.1016/j.tsf.2014.12.036

L. Zheng, Y. Xu, D. Jin, Y. Xie, Novel metastable hexagonal MoO3 nanobelts: synthesis, photochromic and electrochromic properties. Chem. Mater. 21, 5681–5690 (2009)

C.L. Liu, Y. Wang, C. Zhang, X.S. Li, W.S. Dong, In situ synthesis of α-MoO3/graphene composites as anode materials for lithium ion battery. Mater. Chem. Phys. 143, 1111–1118 (2014)

P. Vivek, J. Chandrasekaran, R. Marnadu, S. Maruthamuthu, V. Balasubramani, Incorporation of Ba2+ ions on the properties of MoO3 thin films and fabrication of positive photo-response Cu/Ba–MoO3/p-Si structured diodes. Superlattices Microstructure 133, 106197 (2019)

K.A. Gesheva, T. Ivanova, A low-temperature atmospheric pressure CVD process for growing thin flms of MoO3 and MoO3-WO3 for electrochromic device applications. Chem. Vap. Depos. 12, 231–238 (2006)

K. Galatsis, Y.X. Li, W. Wlodarski, K. Kalantar-zadeh, Sol-gel prepared MoO3-WO3 thin films for O2 gas sensing. Sens. Actuators B 77, 478–483 (2001)

B. Kannan, R. Pandeeswari, B.G. Jeyaprakash, Infuence of precursor solution volume on the properties of spray deposited α-MoO3 thin films. Ceram. Int. 40, 5817–5823 (2014)

M.B. Rahmani, S.H. Keshmiri, J. Yu, A.Z. Sadek, L. Al-Mashat, A. Moaf, K. Latham, Y.X. Li, W. Wlodarski, K. Kalantarzadeh, Gas sensing properties of thermally evaporated lamellar MoO3. Sens. Actuators B 145, 13–19 (2010)

K. Gesheva, A. Cziraki, T. Ivanova, A. Szekeres, Structure and composition of thermally annealed Mo- and W-based CVD metal oxide thin films. Thin Solid Films 492, 322–326 (2005)

X. Zhao, Z. Wu, D. Guo, W. Cui, P. Li, Y. An, L. Li, W. Tang, Growth and characterization of α-phase Ga2–xSnxO3 thin films for solar-blind ultraviolet applications. Semicond. Sci. Technol. 31(1–6), 065010 (2016)

A.R. Babar, P.R. Deshamukh, R.J. Deokate, D. Haranath, C.H.Bhosale, K.Y. Rajpure, Gallium doping in transparent conductive ZnO thin films prepared by chemical spray pyrolysis. J. Phys. D: Appl. Phys. 41(1–6), 135404 (2008)

D. Zhou, F. Shi, D. Xie, D.H. Wang, X.H. Xia, X.L. Wang, C.D. Gu, J.P. Tu, Bi-functional Mo-doped WO3 nanowire array electrochromism-plus electrochemical energy storage. J. Colloid Interface Sci. (2015). https://doi.org/10.1016/j.jcis.2015.11.068.

M. Thambidurai, N. Muthukumarasamy, S. Agilan, N. Murugan, N. Sabari Arul, S. Vasantha, R. Balasundaraprabhu, Studies on optical absorption and structural properties of Fe doped CdS quantum dots, Solid State Sci. 12, 1554–1559 (2010).

P. Scherrer, Bestimmung der Grösse und der inneren Struktur von Kolloidteilchen mittels Rontgenstrahlen. Nachr. Ges. Wiss. Gottingen 26, 98 (1918)

M. Balaji, J. Chandrasekaran, M. Raja, Role of substrate temperature on MoO3 thin films by the JNS pyrolysis technique for p-n junction diode application. Mater. Sci. Semicond. Process. 43,104–113 (2016)

M. Balaji, J. Chandrasekaran, M. Raja, S. Rajesh, Structural, optical and electrical properties of Ru doped MoO3 thin films and its p–n diode application by JNS pyrolysis technique. J. Mater.Sci.: Mater. Electron. (2016).

J. Saju, O.N. Balasundaram, Optimization and characterization of NiO thin flms prepared via NSP technique and its p–n junction diode application. Mater. Sci. Poland 37(3), 338–346 (2019)

L.R. Canfeld, R. Vest, T.N. Woods, R. Korde, Silicon photodiodes with integrated thin film filters for selective bandpasses in the extreme ultraviolet. Ultraviolet Tech. V 2282, 31–38 (1994).

S.K. Cheung, N.W. Cheung, Extraction of Schottky diode parameters from forward current-voltage characteristics. Appl. Phys.Lett. 49, 85 (1986)